the plant journal
SEB Society for Experimental Biology

The Plant Journal (2014) 79, 835–847 doi: 10.1111/tpj.12591

The powdery mildew resistance protein RPW8.2 is carried on VAMP721/722 vesicles to the extrahaustorial membrane of haustorial complexes

Hyeran Kim[1], Richard O'Connell[1,†], Makoto Maekawa-Yoshikawa[1], Tomohiro Uemura[2], Ulla Neumann[3] and Paul Schulze-Lefert[1,*]

[1]Department of Plant Microbe Interactions, Max-Planck-Institute for Plant Breeding Research, Cologne 50829 Germany,
[2]Department of Biological Sciences, Graduate School of Science, University of Tokyo, Bunkyo-ku, Tokyo 113-0033, Japan, and
[3]Central Microscopy, Max-Planck-Institute for Plant Breeding Research, Cologne 50829, Germany

Received 5 March 2014; revised 4 June 2014; accepted 9 June 2014; published online 18 June 2014.
*For correspondence (e-mail schlef@mpipz.mpg.de).
†Present address: UMR1290 BIOGER-CPP, INRA-AgroParisTech, 78850 Thiverval-Grignon, France.

SUMMARY

Plants employ multiple cell-autonomous defense mechanisms to impede pathogenesis of microbial intruders. Previously we identified an exocytosis defense mechanism in Arabidopsis against pathogenic powdery mildew fungi. This pre-invasive defense mechanism depends on the formation of ternary protein complexes consisting of the plasma membrane-localized PEN1 syntaxin, the adaptor protein SNAP33 and closely sequence-related vesicle-resident VAMP721 or VAMP722 proteins. The *Arabidopsis thaliana* resistance to powdery mildew 8.2 protein (RPW8.2) confers disease resistance against powdery mildews upon fungal entry into host cells and is specifically targeted to the extrahaustorial membrane (EHM), which envelops the haustorial complex of the fungus. However, the secretory machinery involved in trafficking RPW8.2 to the EHM is unknown. Here we report that RPW8.2 is transiently located on VAMP721/722 vesicles, and later incorporated into the EHM of mature haustoria. Resistance activity of RPW8.2 against the powdery mildew *Golovinomyces orontii* is greatly diminished in the absence of VAMP721 but only slightly so in the absence of VAMP722. Consistent with this result, trafficking of RPW8.2 to the EHM is delayed in the absence of VAMP721. These findings implicate VAMP721/722 vesicles as key components of the secretory machinery for carrying RPW8.2 to the plant–fungal interface. Quantitative fluorescence recovery after photobleaching suggests that vesicle-mediated trafficking of RPW8.2–yellow fluorescent protein (YFP) to the EHM occurs transiently during early haustorial development and that lateral diffusion of RPW8.2–YFP within the EHM exceeds vesicle-mediated replenishment of RPW8.2–YFP in mature haustoria. Our findings imply the engagement of VAMP721/722 in a bifurcated trafficking pathway for pre-invasive defense at the cell periphery and post-invasive defense at the EHM.

Keywords: VAMP721/722 vesicles, RPW8.2 trafficking, haustorial complex, extrahaustorial membrane, vesicle trafficking, secretion, plant–fungal interface, Arabidopsis, *Golovinomyces orontii*, Exocytosis.

INTRODUCTION

Powdery mildew fungi (Ascomycotina, Erysiphales) are obligate biotrophic pathogens, requiring a living host plant for their growth and reproduction, and they cause disease on about 10 000 angiosperm species, including barley, wheat, cucurbits, grapes and tree fruits, as well as the model plant Arabidopsis (Micali *et al*., 2008). Conidiospores germinating on the surface of the plant leaf produce appressoria, which break through the plant cuticle and cell wall to form specialized feeding structures called haustoria inside the living epidermal cells of the plant. Subsequently these fungi proliferate extensively on the leaf surface as a branched epiphytic mycelium that produces further secondary haustoria and finally sporulating structures, i.e. conidiophores and conidiospores (Xiao *et al*., 2001; Micali *et al.*, 2008). During invasion of host cells haustoria become enveloped by a highly modified host-derived membrane, the extrahaustorial membrane (EHM), which separates the haustorium from the host cytoplasm. The EHM provides a pivotal interface for the uptake of nutrients and water from the host and for the delivery of effector proteins secreted by the fungus to manipulate host cells (Bozkurt *et al.*, 2011; Caillaud *et al.*, 2012). The EHM is continuous with the plant plasma membrane but has a markedly different structure and composition. Thus, with transmission electron microscopy, the EHM appears thicker and more convoluted than the normal plasma membrane and lacks biochemical markers such as ATPase activity (Gil and Gay, 1977; Spencer-Phillips and Gay, 1981; Micali *et al.*, 2011). More recent cell biological studies have revealed that many plant plasma membrane proteins are also excluded from the EHM (Koh *et al.*, 2005; Meyer *et al.*, 2009; Micali *et al.*, 2011). Based on these findings, two models for EHM biogenesis were proposed, namely invagination of the plasma membrane followed by membrane differentiation or *de novo* synthesis by means of targeted vesicle trafficking (Koh *et al.*, 2005). However, despite many advances in our understanding of protein trafficking pathways in plant cells, the mechanism of EHM biogenesis remains obscure.

The Arabidopsis genome encodes 60 SNARE (soluble *N*-ethylmaleimide-sensitive factor adaptor protein receptors) family members which are grouped into four subtypes, denoted as Qa, Qb, Qc and R-SNAREs. The R-SNARE subfamily consists of 15 members assigned to four sequence-diversified groups, designated VAMP71s, VAMP72s, YKT6s and SEC22s (Lipka *et al.*, 2007). Previously we showed that the vesicle-resident R-SNARE proteins VAMP721/722 form a ternary SNARE complex together with the plasma membrane-resident PEN1 Qa SNARE (syntaxin) and the adaptor protein Qb+Qc SNARE SNAP33 that is required for vesicle-mediated immune responses (Kwon *et al.*, 2008). VAMP721/722 proteins are also found at the cell plate during the cytokinesis of Arabidopsis root cells (Zhang *et al.*, 2011). VAMP721/722 vesicles probably originate from the *trans*-Golgi network (TGN), where they partly co-localize with SYP43 protein, a Qa SNARE resident at the TGN (Uemura *et al.*, 2012). Recently it was reported that VAMP721/722 vesicles are required for sustained plant growth during immune responses and following application of exogenous ABA (Yi *et al.*, 2013; Yun *et al.*, 2013). Although VAMP721/722 proteins are known to be functionally redundant for extracellular immune responses, there are some clues suggesting they have distinct functions in plant defense. Thus, *VAMP721*$^{-/-}$ *VAMP722*$^{+/-}$ mutant plants showed hypersusceptibility to the oomycete pathogen *Hyaloperonospora parasitica*, while *VAMP721*$^{+/-}$ *VAMP722*$^{-/-}$ mutant plants showed an increased frequency of host cell entry by the non-adapted powdery mildew fungus *Erysiphe pisi* (Kwon *et al.*, 2008). However, it is unknown which molecular cargos are carried by VAMP721/722 vesicles for the execution of defense responses.

The *Arabidopsis thaliana* resistance to powdery mildew proteins RPW8.1 and RPW8.2 were first identified in Arabidopsis accession Ms-0 and shown to confer broad-spectrum resistance to diverse species of powdery mildew fungi (Xiao *et al.*, 2001; Wang *et al.*, 2007). RPW8.1 and RPW8.2 are 18–20 kDa proteins comprising a predicted N-terminal transmembrane domain and one to two coiled-coil domain(s) (Xiao *et al.*, 2001). As such, they represent a class of atypical resistance (R) proteins that show no obvious similarity to the intracellular nucleotide-binding domain and leucine-rich repeat (NLR) family of plant R proteins mediating pathogen effector-triggered immunity (ETI) (Xiao *et al.*, 2001; Maekawa *et al.*, 2011). However, RPW8.1 and RPW8.2 resistance proteins share with a subset of NLRs the engagement of the regulatory lipase-like protein EDS1 for the function of disease resistance and activation of a host cell death response (Xiao *et al.*, 2001). The transcription of *RPW8.2* is highly induced upon infection by powdery mildew fungi and the protein becomes specifically targeted to the EHM during differentiation of the haustorium, where it mediates highly localized defense responses such as encasement of the haustorium by callose and accumulation of H_2O_2 at the haustorial interface (Wang *et al.*, 2009). In common with ETI, these haustorium-focused defenses mediated by RPW8.2 are dependent on EDS1 and the SA-signaling pathway (Xiao *et al.*, 2001, 2003).

Based on a comprehensive mutational analysis, it was recently shown that specific targeting of RPW8.2 to the EHM requires two short motifs (R/K-R/K-xR/K) and an N-terminal transmembrane domain, which together define a minimal 60 amino acid core-targeting motif (Wang *et al.*, 2013). Using fluorescent protein tagging, RPW8.2 and versions of the protein mutated in this core-targeting motif were detected in unidentified vesicle-like structures in the host cytoplasm (Wang *et al.*, 2009, 2013). In a previous study on *Golovinomyces orontii* haustoria, we also showed that RPW8.2–yellow fluorescent protein (YFP) is incorporated into the EHM in a time-dependent manner, with the fusion protein abundant in the EHM around fully expanded haustoria (Micali *et al.*, 2011). In the present study, we used a combination of genetic and cell biological approaches to show that RPW8.2 is initially carried on VAMP721/722 vesicles, and that VAMP721, and to a much lesser extent VAMP722, are essential for transporting RPW8.2 to the EHM and for the defense activity of RPW8.2. Thus, VAMP721/722 vesicles are revealed to be key components of a secretory pathway that specifically carries RPW8.2, and possibly other protein and lipid components, to the EHM.

RESULTS

RPW8.2 is targeted to the EHM upon infection by *G. orontii*

To monitor the dynamics of RPW8.2 trafficking in Arabidopsis leaf epidermal cells upon inoculation with the host-adapted powdery mildew *G. orontii*, we generated transgenic lines expressing RPW8.2–YFP under the native promoter, using a construct described previously (Wang *et al.*, 2007). Following inoculation of 4-week-old plants with *G. orontii* conidiospores, we found that RPW8.2–YFP first appeared at sites of attempted fungal entry at about 18 h post-inoculation (hpi), when small, punctate vesicle-like structures were visible in the cytoplasm of infected epidermal cells. RPW8.2–YFP labeled punctate structures were more numerous and appeared concentrated in the cytoplasm around haustoria at 24 hpi (Figure 1a). At 48 hpi, the RPW8.2–YFP fusion protein strongly labeled the EHM of fully mature haustoria (Figure 1b), but the number of labeled punctate structures in haustoria-containing cells was dramatically reduced or not detectable at this stage. The specific localization of RPW8.2 proteins in the EHM of *G. orontii* haustoria was confirmed using the higher resolution of TEM immunogold labeling with transgenic plants expressing RPW8.2-RFP and anti-RFP antibodies (Figure 1c, d, Figure S1 in Supporting Information, Methods S1) (Sarnowska *et al.*, 2013).

RPW8.2 transiently co-localizes with VAMP721/722 vesicles

To obtain insight into the nature of the secretory machinery required for trafficking RPW8.2 protein to the EHM, we investigated the identity of the punctate structures visible in the early stages of haustorium formation. In our previous studies (Kwon *et al.*, 2008; Yun *et al.*, 2013), VAMP721/722 vesicles were shown to act as functionally overlapping

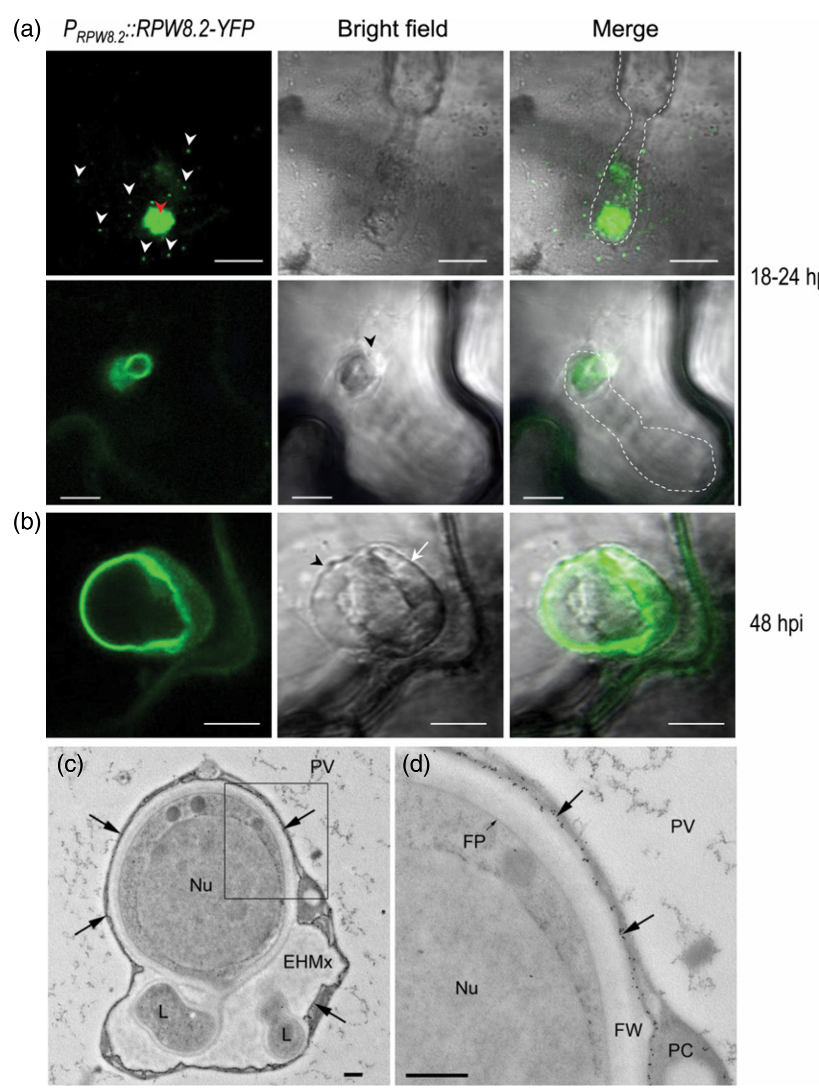

Figure 1. Trafficking of RPW8.2 protein to the extrahaustorial membrane (EHM) upon *Golovinomyces orontii* infection.
(a), (b) Confocal microscope images from single optical sections of Arabidopsis leaf epidermal cells expressing RPW8.2-YFP infected by *G. orontii*. The yellow fluorescent protein (YFP) fluorescence is presented in green. White dashed lines outline *G. orontii* conidiospores and appressoria. Scale bars = 10 μm. (a) 18 hours post-inoculation (hpi) to 24 hpi. Focal accumulation of RPW8.2–YFP beneath the fungal appressorium corresponds to a callose papilla formed at the penetration site (red arrowhead). Note numerous punctate, vesicle-like structures in the cytoplasm of infected epidermal cells are labeled by RPW8.2–YFP (white arrowheads). The EHM (black arrowhead) of a young, expanding haustorium is strongly labeled by RPW8.2–YFP.
(b) 48 hpi. The EHM (black arrowhead) around a mature, fully expanded haustorium is strongly labeled by RPW8.2–YFP. The haustorial encasement (white arrow) is also weakly labeled.
(c), (d) Transmission electron microscopy immunogold images showing an Arabidopsis cotyledon epidermal cell expressing RPW8.2–RFP infected by a mature haustorium of *G. orontii* at 48 hpi. (c) Overview and (d) an enlargement of the boxed region in (c). The extrahaustorial membrane (arrows) is specifically labeled by anti-RFP antibody. The haustorium is surrounded by a thin layer of plant cytoplasm (PC). FW, fungal cell wall; EHMx, extrahaustorial matrix; FP, fungal plasma membrane; L, haustorial lobe; Nu, nucleus; PV, plant vacuole. Scale bars: 500 nm.

components of a vesicle-mediated exocytosis pathway that is involved in disease resistance to the non-adapted powdery mildew *Blumeria graminis* and *Erysiphe pisi* and the host-adapted powdery mildew *G. orontii*. These VAMP721 and VAMP722 proteins were reported to be localized on mobile, punctate structures inside host cells. To examine whether the punctate structures labeled by RPW8.2–YFP are the same, we generated transgenic plants co-expressing RPW8.2–YFP (Wang *et al.*, 2007) and mRFP-VAMP722 (Uemura *et al.*, 2012) under their respective, native 5′ regulatory sequences. Remarkably, at early infection stages (18–24 hpi) RPW8.2–YFP and mRFP–VAMP722 were transiently co-localized at the same punctate vesicle-like structures in infected epidermal cells (Figures 2a and S2). The co-localized structures were distributed throughout the infected cell, from the incipient entry site beneath the fungal appressorium to the much deeper focal planes containing the haustorial body. At those focal planes providing a cross-section through the haustorium (orientation as shown in the inset to Figure 2a), RPW8.2–YFP and mRFP–VAMP722, respectively, labeled discrete inner and outer regions of the haustorial complex. Thus, RPW8.2–YFP labeled the EHM near the haustorial neck while mRFP–VAMP722 labelled the surrounding haustorial encasement. In cells containing fully mature haustoria at 48 hpi, RPW8.2–YFP proteins were strongly incorporated into the EHM as well as the haustorial encasement. In contrast, mRFP–VAMP722 proteins were incorporated into the

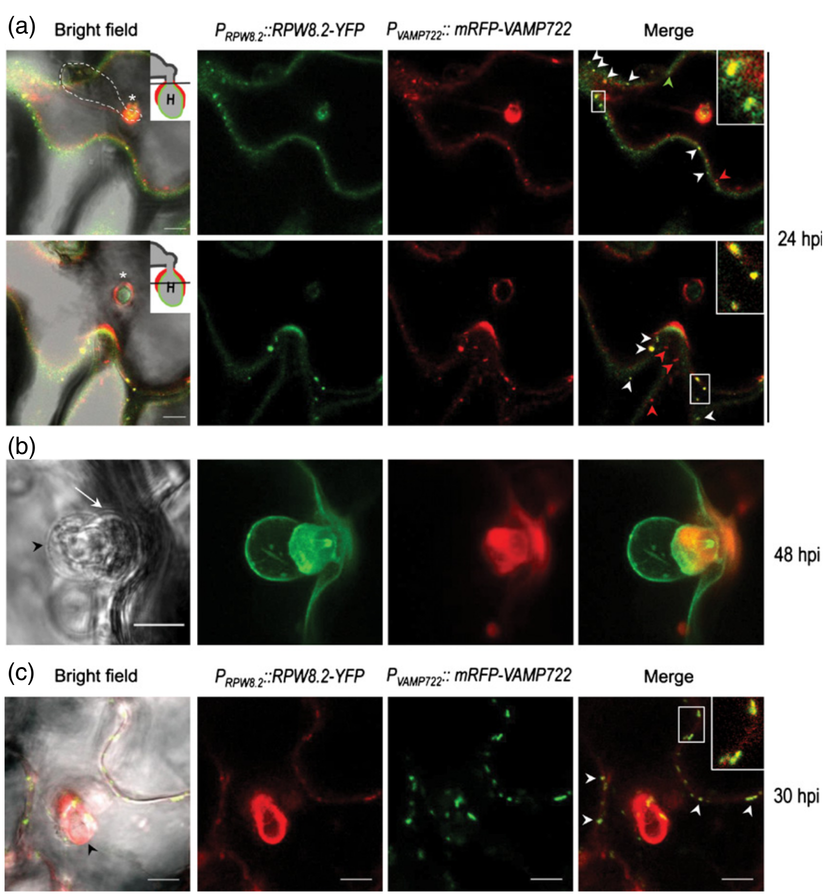

Figure 2. Transient co-localization of RPW8.2 with VAMP721/722 vesicles and their targeting at haustorial complexes.
Confocal microscope images of *Golovinomyces orontii* infecting Arabidopsis leaf epidermal cells co-expressing either RPW8.2-YFP (green)/mRFP-VAMP722 (red) or RPW8.2-RFP (red)/GFP-VAMP721 (green). Insets in the merged panel correspond to an enlarged region of co-localized structures in the main image. Scale bars = 10 μm.
(a) RPW8.2–YFP proteins are transiently carried on mRFP–VAMP722 labeled vesicles during invasive growth of *G. orontii* at 24 h post-infection (hpi). White dashed lines outline the *G. orontii* conidiospore and appressorium. Cartoon insets indicate the approximate position of the single optical sections presented in (a) in relation to the haustorium (H, white asterisk; extrahaustorial membrane green; haustorial encasement red). White arrowheads indicate vesicles where RPW8.2–YFP and mRFP–VAMP722 co-localize, green arrowheads indicate vesicles labeled only by RPW8.2–YFP and red arrowheads indicate vesicles labeled only by mRFP–VAMP722.
(b) Fully expanded haustorium of *G. orontii* at 48 hpi. After arrival at the haustorium, RPW8.2–YFP proteins are incorporated into the extrahaustorial membrane (EHM; black arrowhead) and the extrahaustorial encasement (white arrow), while mRFP-VAMP722 proteins are incorporated into the encasement only.
(c) RPW8.2–RFP proteins are transiently carried on GFP–VAMP721 labeled vesicles during invasive growth of *G. orontii* and incorporated into the EHM (black arrowhead) at 30 hpi. White arrowheads indicate vesicles on which RPW8.2–RFP and GFP–VAMP722 co-localize.

encasement but not the EHM (Figure 2b). Similarly, in transgenic plants co-expressing RPW8.2–RFP (Wang *et al*., 2007) and GFP–VAMP721 (Ebine *et al*., 2011) under their respective native 5′ regulatory sequences, the fusion proteins also co-localized at punctate vesicle-like structures in epidermal cells containing young haustoria of *G. orontii* at 30 hpi (Figure 2c). Taken together, these data demonstrate that RPW8.2 proteins are transiently carried to the EHM on VAMP721/722 vesicles during infection by *G. orontii*.

To determine whether trafficking of RPW8.2 protein depends on VAMP721/722 gene dosage, we also generated RPW8.2–YFP expressing transgenic lines by introducing the corresponding transgene independently in the genetic background of *VAMP721*$^{-/-}$ *VAMP722*$^{+/-}$ and *VAMP721*$^{+/-}$ *VAMP722*$^{-/-}$ haploinsufficiency mutations. Before analyzing the localization of RPW8.2, we first evaluated the pathogenicity of *G. orontii* on *VAMP721*$^{-/-}$ *VAMP722*$^{+/-}$ and *VAMP721*$^{+/-}$ *VAMP722*$^{-/-}$ mutants. To successfully complete its life cycle on an Arabidopsis leaf, germinating conidiospores and appressoria of *G. orontii* must first penetrate the cell wall of leaf epidermal cells to establish primary haustoria by invagination of the host plasma membrane, then proliferate on the leaf surface as an epiphytic branching mycelium producing further secondary haustoria, and finally produce sporulating structures for asexual reproduction, i.e. conidiophores and conidiospores (Micali *et al*., 2011). To evaluate pathogenicity on different host genotypes, we quantified the frequency with which fungal appressoria successfully entered host epidermal cells to form visible primary haustoria (fungal entry rate) and we also counted the number of conidiospores per gram fresh weight of leaf tissue (reproductive fitness). Upon inoculation of *G. orontii* on *VAMP721*$^{-/-}$ *VAMP722*$^{+/-}$ and *VAMP721*$^{+/-}$ *VAMP722*$^{-/-}$ mutants, the fungal entry rate was similar to wild-type Col-0 plants, with an entry rate of about 80% at 24 hpi. (Figure S3). Although we previously described the macroscopic phenotypes of *G. orontii* on both haploinsufficient mutants (Kwon *et al*., 2008), here we quantified the reproductive fitness of *G. orontii* on those mutants, including the *eds1*-2 mutant that lacks an essential component for basal plant immune responses as a hypersusceptible control (Aarts *et al*., 1998). Consistent with previous macroscopic observations, sporulation of *G. orontii* on the *VAMP721*$^{-/-}$ *VAMP722*$^{+/-}$ mutant was slightly enhanced compared with the wild type at 7 days post-inoculation (dpi), although this was not statistically significant by ANOVA analysis. Plants of the other mutant genotype, *VAMP721*$^{+/-}$ *VAMP722*$^{-/-}$, also supported enhanced sporulation at 10 dpi, but in this case the difference was significant ($P < 0.01$) by ANOVA analysis (Figure 3a).

To evaluate the effect of RPW8.2 on resistance to *G. orontii*, we examined fungal sporulation phenotypes on transgenic plants expressing RPW8.2–YFP compared with Col-0 wild type plants. Upon *G. orontii* challenge, the leaves of

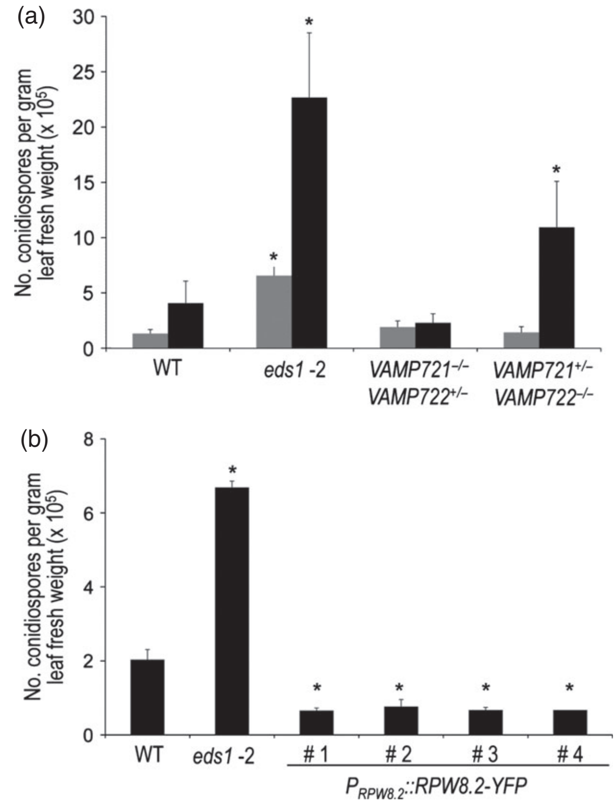

Figure 3. VAMP721/VAMP722 gene dosage and RPW8.2–YFP affect post-invasion resistance to *Golovinomyces orontii*.
(a) Quantification of *G. orontii* sporulation (number of conidiospores per gram leaf fresh weight) on the indicated plant genotypes at 7 days post-inoculation (dpi) (grey bars) and 10 dpi (black bars).
(b) Quantification of *G. orontii* sporulation at 7 dpi on four independent Arabidopsis transgenic lines expressing RPW8.2–YFP.
Bars represent the mean ± standard deviation of three samples (300 mg of four plants each). The asterisk indicates ANOVA, $P < 0.01$ compared with wild-type (WT) plants. The *eds1*-2 mutant provides a hypersusceptible control for the growth of *G. orontii.*

RPW8.2–YFP-expressing plants developed necrotic lesions without macroscopically visible white, powdery spores (Figure S4) as reported previously for *Golovinomyces cichoracearum* UCSC1 (Wang *et al*., 2009). We further quantified *G. orontii* sporulation with four independent transgenic lines expressing RPW8.2–YFP. At 7 dpi, the examined RPW8.2–YFP transgenic plants supported less *G. orontii* sporulation (about 30% of wild type) (Figure 3b), confirming earlier reports that *RPW8.2* derived from the resistant Arabidopsis ecotype Ms-0 is necessary and sufficient to confer quantitative disease resistance when expressed as a fluorescent fusion protein in the susceptible Col-0 ecotype (Wang *et al*., 2007).

The resistance function of RPW8.2 is diminished in the absence of VAMP721 but not VAMP722

To understand the genetic interaction between trafficking of RPW8.2 to the EHM and the resistance function of the protein, we compared sporulation of *G. orontii* on two independent transgenic plants each of *RPW8.2–YFP VAMP721*$^{-/-}$ *VAMP722*$^{+/-}$ and *RPW8.2–YFP VAMP721*$^{+/-}$ *VAMP722*$^{-/-}$, including Col-0 wild type and *eds1*-2 as controls. Macroscopically, *RPW8.2–YFP VAMP721*$^{+/-}$ *VAMP722*$^{-/-}$ transgenic plants showed obvious leaf chlorosis. In contrast, *RPW8.2-YFP VAMP721*$^{-/-}$ *VAMP722*$^{+/-}$ transgenic plants displayed visible white, powdery fungal growth similar to the Col-0 wild type (Figure 4a). To substantiate these infection phenotypes, we observed the infected leaves of each genotype with scanning electron microscopy. Wild type and *eds1*-2 plants had profuse fungal mycelia with conidiophores and conidiospores. Consistently, *RPW8.2–YFP VAMP721*$^{-/-}$ *VAMP722*$^{+/-}$ plants also supported copious fungal mycelium with conidiophores and conidiospores. However, in contrast to the other genotypes, *RPW8.2–YFP VAMP721*$^{+/-}$ *VAMP722*$^{-/-}$ plants had only fungal mycelium on the leaf surface without conidiospores (Figures 4b and S6, Methods S2). To quantify the reproductive fitness of *G. orontii* on each genotype, we harvested 300 mg of infected leaf material to count the fungal conidiospores at 10 dpi. In addition, to take account of potential integration site-dependent variation in *RPW8.2–YFP* transgene expression, we generated four independent transgenic lines expressing *RPW8.2–YFP* in the haploinsufficient backgrounds (Figure 4c, lines #16 and #21 in *VAMP721*$^{-/-}$ *VAMP722*$^{+/-}$ and #27 and #34 in *VAMP721*$^{+/-}$ *VAMP722*$^{-/-}$). We selected siblings of these lines expressing *RPW8.2–YFP* from the same integration sites in *vamp721* or *vamp722* single mutant backgrounds. Consistent with the macroscopic and microscopic phenotypes (Figure 4a, b), sporulation of *G. orontii* on the independent transgenic lines of *RPW8.2–YFP VAMP721*$^{+/-}$ *VAMP722*$^{-/-}$ (#27, #34) was significantly reduced (17 and 3% of that on wild-type plants) (Figure 4c). Remarkably, conidiospore counts on RPW8.2–YFP *VAMP721*$^{-/-}$ *VAMP722*$^{+/-}$ plants (#16, #21) were comparable to wild type (Figure 4c). Thus, the function of Arabidopsis resistance protein RPW8.2–YFP

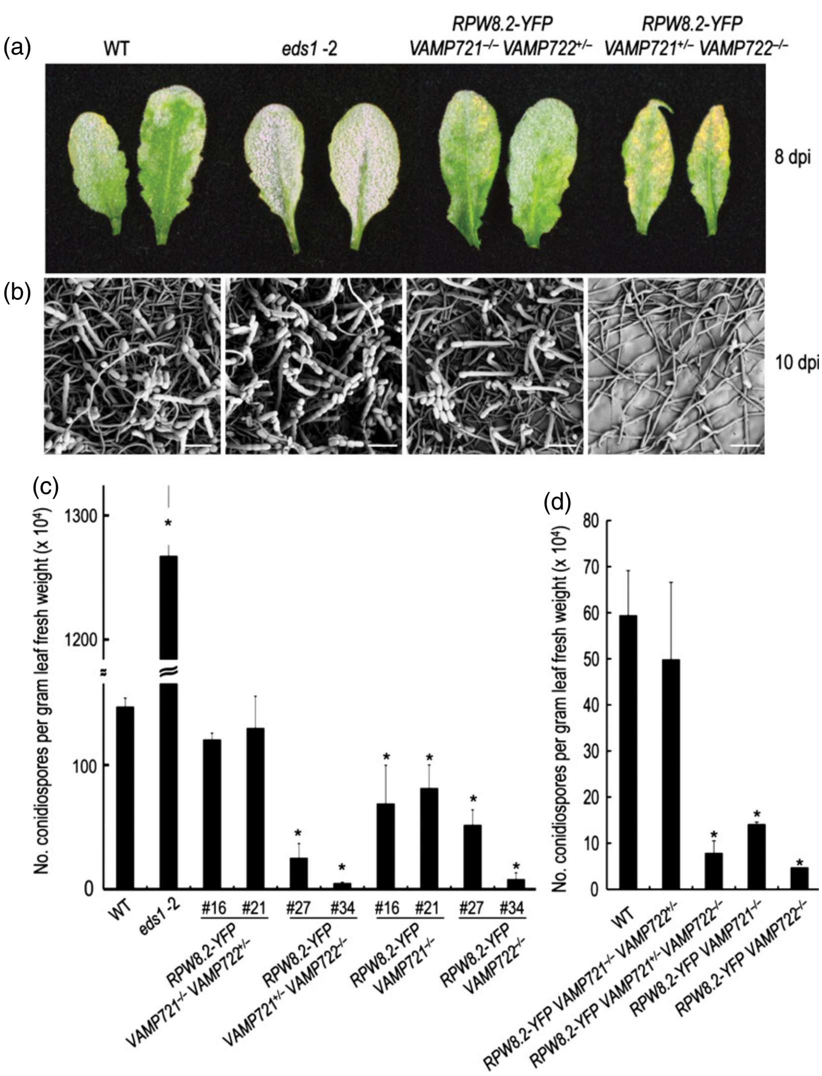

Figure 4. The resistance function of RPW8.2–YFP is diminished in the absence of VAMP721, but not VAMP722.
(a) Macroscopic symptoms of *Golovinomyces orontii* growth on plants expressing RPW8.2–YFP in *VAMP721*$^{-/-}$ *VAMP722*$^{+/-}$ and *VAMP721*$^{+/-}$ *VAMP722*$^{-/-}$ mutant backgrounds, 8 days post-inoculation (dpi).
(b) Cryo-scanning electron micrographs showing epiphytic mycelium and conidiophores of *G. orontii* on the indicated plant genotypes at 10 dpi. Scale bars = 50 μm.
(c) Quantification of *G. orontii* sporulation at 10 dpi on the indicated plant genotypes (two independent transgenic lines per genotype). Bars represent the mean ± standard deviation of four samples (300 mg of four plants each).
(d) Quantification of *G. orontii* sporulation at 7 dpi on the indicated plant genotypes with the same integration site for RPW8.2 expression in the haploinsufficient mutant backgrounds and in the Col-0 wild-type, RPW8.2-YFP Col-0 transgenic lines #3 and #4 (Figure 3b) were crossed with both haploinsufficient mutants.
Bars represent the mean ± standard deviation of three samples (two independent lines each). Asterisk indicates ANOVA, $P < 0.01$ compared with Col-0 wild-type plants.

was greatly diminished in the absence of VAMP721 but only slightly so in the absence of VAMP722. Strikingly, both *vamp721* and *vamp722* single mutant siblings expressing RPW8.2–YFP still retained the resistance function of RPW8.2–YFP (Figure 4c). To verify that the expression levels of RPW8.2–YFP protein were similar in both haploinsufficient mutants, we purified total proteins from *G. orontii*-infected leaves for Western blot analysis. Yellow fluorescent protein fused to RPW8.2 protein of the predicted size was detected with similar abundance in all the transgenic plants using anti-GFP antibodies, whereas VAMP722 protein accumulated differentially according to *VAMP722* dosage (Figure S5; note that the anti-VAMP722 antibody cross-reacts with VAMP721, which is a similar size to VAMP722).

We devised an additional genetic test to corroborate the preferential requirement of VAMP721 for RPW8.2-mediated disease resistance activity. We crossed two independent RPW8.2–YFP expressing transgenic lines generated in the Col-0 wild-type background (lines #3 and #4 in Figure 3b) with both haploinsufficient mutants and selected among the F_2 progeny those siblings expressing RPW8.2–YFP in *vamp721* or *vamp722* single-mutant backgrounds or both haploinsufficient mutant backgrounds (Figure 4d). The reproductive fitness of *G. orontii* on these host genotypes was quantified by conidiospore counts at 7 dpi. Consistent with the aforementioned genetic test for the role of *VAMP721/722* in *RPW8.2*-mediated disease resistance (Figure 4c), reproductive fitness of the pathogen on *VAMP721*$^{-/-}$ *VAMP722*$^{+/-}$ plants was similar to wild type, whereas on *VAMP721*$^{+/-}$ *VAMP722*$^{-/-}$ plants sporulation was significantly reduced (13% of wild type levels; Figure 4d). Sporulation of *G. orontii* on *vamp721* and *vamp722* single mutant plants was drastically reduced (24 and 8% of wild type, respectively; Figure 4d). Taken together, the findings of both genetic tests suggest that VAMP721 is more critical for the resistance function of RPW8.2 than VAMP722.

RPW8.2 trafficking to the EHM is delayed by reduced gene dosage of *VAMP721* and *VAMP722*

To obtain insight into the phenotype of copious *G. orontii* sporulation on *RPW8.2–YFP VAMP721*$^{-/-}$ *VAMP722*$^{+/-}$ transgenic plants, we investigated whether trafficking of RPW8.2 protein to the EHM is differentially affected in the *RPW8.2–YFP VAMP721*$^{-/-}$ *VAMP722*$^{+/-}$ and *RPW8.2–YFP VAMP721*$^{+/-}$ *VAMP722*$^{-/-}$ plants. In the background of *VAMP721*$^{+/-}$ *VAMP722*$^{-/-}$, RPW8.2 protein was properly targeted to haustorial complexes at 2 dpi. However, in the background of *VAMP721*$^{-/-}$ *VAMP722*$^{+/-}$, RPW8.2 protein remained at the cell periphery and was not detectable at the haustorial complex at 2 dpi (Figure 5a). The delayed trafficking of RPW8.2 protein in *VAMP721*$^{-/-}$ *VAMP722*$^{+/-}$ plants also persisted at 6 dpi but could not be quantified because at

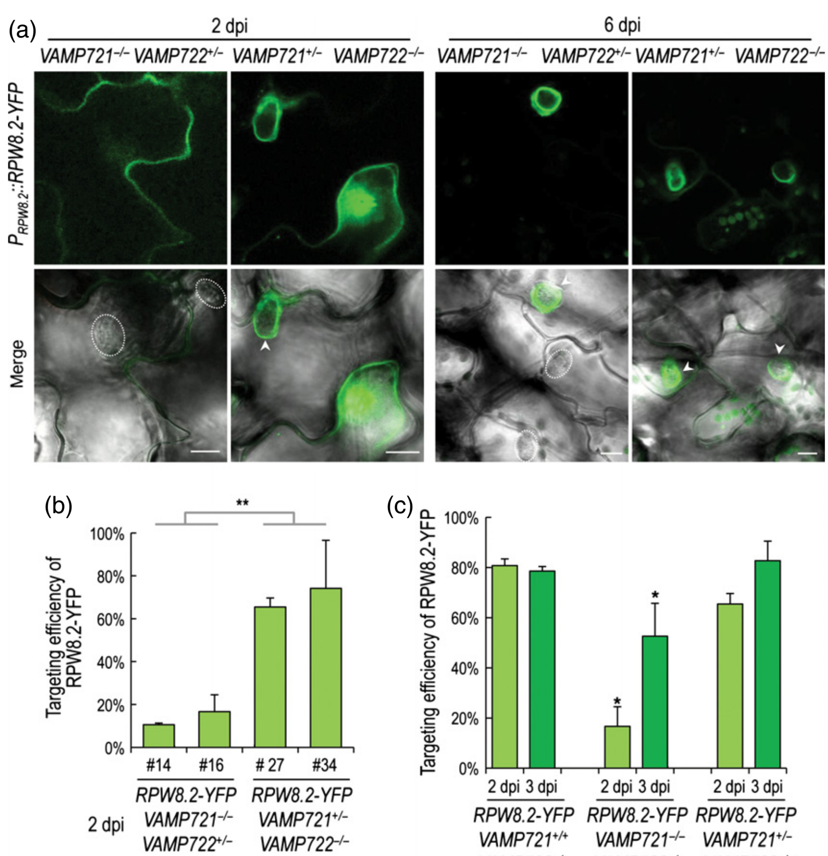

Figure 5. Reduced VAMP721/722 gene dosage delays trafficking of RPW8.2-YFP to *Golovinomyces orontii* haustoria.
(a) Confocal microscope images of *G. orontii* infecting Arabidopsis leaf epidermal cells expressing RPW8.2–yellow fluorescent protein (YFP) (shown in green) in *VAMP721*$^{-/-}$ *VAMP722*$^{+/-}$ and *VAMP721*$^{+/-}$ *VAMP722*$^{-/-}$ mutant backgrounds at 2 and 6 days post-inoculation (dpi). White dotted ellipses outline unlabeled *G. orontii* haustoria. White arrowheads indicate the RPW8.2–YFP-labelled extrahaustorial membrane. Scale bars = 10 μm.
(b), (c) Quantification of haustoria labeled by RPW8.2–YFP at 2 and/or 3 dpi. Data represent the mean proportion of haustoria labeled by RPW8.2–YFP at 2 dpi (light green bars) and at 3 dpi (dark green bars), based on at least three independent experiments, with a total of 60 or more mature haustoria examined per genotype per time point. At least two independent transgenic lines were examined for each plant genotype. ** and * denote significant differences in the indicated comparisons ($P < 0.001$, Student's *t*-test and $P < 0.01$, ANOVA, respectively).

this stage the tissue contained a mixture of primary and secondary haustoria at different stages of development. Overall these results correlated with the phenotype of enhanced *G. orontii* sporulation on *RPW8.2–YFP VAMP721*$^{-/-}$ *VAMP722*$^{+/-}$ plants.

To quantify the observed delay in RPW8.2 trafficking, we counted RPW8.2–YFP-labeled and unlabeled haustorial complexes on each genotype. *RPW8.2–YFP VAMP721*$^{-/-}$ *VAMP722*$^{+/-}$ plants contained 11 or 16% of labeled haustorial complexes in two independent transgenic plants (lines #14 and #16) at 2 dpi, whereas *RPW8.2–YFP VAMP721*$^{+/-}$ *VAMP722*$^{-/-}$ plants contained over 65 or 74% of labeled haustorial complexes in two independent transgenic plants (lines #27 and #34) at 2 dpi. The difference between the genotypes was significant ($P < 0.001$) by Student's *t*-test (Figure 5b). To further evaluate the delayed trafficking of RPW8.2–YFP, we examined haustoria at two different time points, namely 2 and 3 dpi, when primary haustoria are mature and fully expanded. In transgenic Col-0 plants expressing *RPW8.2–YFP* in an otherwise wild-type background (denoted as *RPW8.2–YFP VAMP721*$^{+/+}$ *VAMP722*$^{+/+}$ in Figure 5b), 81 and 79% of haustorial complexes displayed a labeled EHM at 2 and 3 dpi, respectively. In contrast, *RPW8.2–YFP VAMP721*$^{-/-}$ *VAMP722*$^{+/-}$ plants carried 17 and 53% of EHM-labeled haustorial complexes at 2 and 3 dpi, respectively. Compared with transgenic *RPW8.2–YFP VAMP721*$^{+/+}$ *VAMP722*$^{+/+}$ control plants, the haustorial targeting efficiency was significantly reduced ($P < 0.01$) at both time points by ANOVA analysis. In contrast, the targeting efficiency in *RPW8.2–YFP VAMP721*$^{+/-}$ *VAMP722*$^{-/-}$ plants (65 and 83% of labeled haustorial complexes at 2 and 3 dpi, respectively) was not significantly different from transgenic *RPW8.2–YFP VAMP721*$^{+/+}$ *VAMP722*$^{+/+}$ control plants (Figure 5b). These findings demonstrate that VAMP721 plays a more important role in the efficient targeting of RPW8.2 to the EHM than does VAMP722. The results are consistent with the genetic analysis of RPW8.2 disease resistance activity upon reduced gene dosage of *VAMP721* and *VAMP722*.

Quantitative fluorescence recovery after photobleaching reveals lateral diffusion of RPW8.2–YFP within the EHM exceeds vesicle-mediated RPW8.2–YFP replenishment

Fluorescence recovery after photobleaching (FRAP) is widely used to quantify the dynamics of fluorescently labeled proteins within cell membranes (Martiniere *et al.*, 2012; Takagi *et al.*, 2013). The fluorescence recovery curve of membrane-resident proteins describes the sum of two additive mechanisms, lateral mobility of the protein within the membrane and the exchange of proteins between cytoplasmic vesicles and the membrane via exocytosis and endocytosis. The recovery of RPW8.2–YFP fluorescence in the EHM after photobleaching was reported for *G. cichoracearum*, demonstrating fluidity of the EHM (Wang *et al.*, 2009). We conducted quantitative FRAP analysis in Arabidopsis leaf epidermal cells expressing RPW8.2–YFP infected by *G. orontii*. To investigate the dynamics of RPW8.2 at the EHM, we conducted quantitative FRAP of young developing haustoria (less than 10 μm) at 24 hpi and mature haustoria (without visible cell wall encasement) at 48 hpi in Arabidopsis leaf epidermal cells expressing RPW8.2–YFP. Data from individual bleaching experiments at these time points were obtained for the region of interest (red box) before and after photobleaching, and for background (white box 1) and an unbleached RPW8.2–YFP reference region (white box 2) (Figure 6a). After bleaching RPW8.2–YFP in the EHM at the distal (apical) portion of the haustorium, the recovery of YFP fluorescence was quantified over time. The EHM-localized RPW8.2–YFP protein was clearly bleached and about 10% of the pre-bleach signal remained after bleaching. The YFP signal gradually recovered over the course of the experiment (10 to 12 min) at the EHM of both 24 and 48 hpi haustoria (Figures S8b and 6a, respectively). The data were analyzed using the easyFRAP tool (Rapsomaniki *et al.*, 2012) for normalization of the raw data and subsequent fitting of the recovery curve to a single exponential for calculating half-maximal recovery time ($t_{1/2}$) and the mobile fraction (Figures 6b, c and S7). To evaluate the background levels of photobleaching caused by repeated confocal scanning, we monitored RPW8.2 fluorescence intensity at the EHM without bleaching over a time course of 10 min. No significant changes in fluorescence intensity were found during acquisition of a series of 40 images at 15-sec intervals (Figure S8a). Based on independent bleaching experiments on 28 individual young haustoria at 24 hpi, we obtained an average $t_{1/2}$ of 207.6 ± 106.2 sec and a mobile fraction of $68.8 \pm 27.2\%$ (Figure 6b). At 48 hpi, the average $t_{1/2}$ of RPW8.2-YFP at the EHM was only slightly lower (198.1 ± 68.4 sec) whereas the mobile fraction was substantially reduced ($51.7 \pm 10.9\%$; Figure 6c). In addition, we noted that the variation in both the mobile fraction and $t_{1/2}$ between individual haustoria was greater at 24 hpi than at 48 hpi. Similarly, we observed greater variation in pre-bleach fluorescence intensity at the EHM at 24 hpi than at 48 hpi (Figures S7c and S8c). The pre-bleach fluorescence intensity and $t_{1/2}$ at 24 hpi showed a moderate positive correlation ($R = 0.63$; Figure S7d). Together these data point towards the existence of a period during early haustorium biogenesis when RPW8.2–YFP is highly dynamic, i.e. the mobile fraction is >70% and $t_{1/2}$ is <100 sec.

To examine more closely the recovery of RPW8.2–YFP fluorescence in the bleached apical EHM region (red box in Figure 6d), we conducted repetitive FRAP experiments with three successive bleachings of the same apical region. This resulted in a progressive decrease in RPW8.2–YFP fluorescence in adjacent non-bleached EHM regions, as illustrated by false color indexing of the fluorescence intensity.

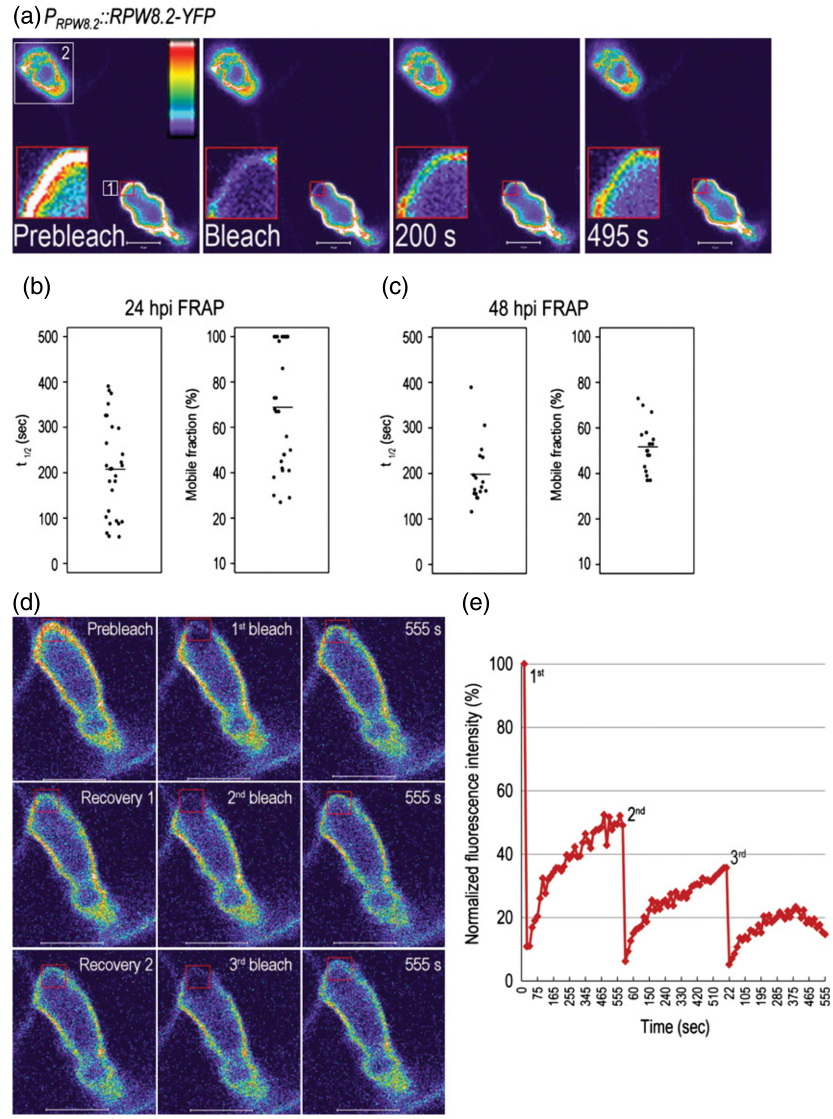

Figure 6. Fluorescence recovery after photobleaching (FRAP) analysis of RPW8.2–yellow fluorescent protein (YFP) dynamics at the extrahaustorial membrane (EHM).
(a) The FRAP images of *Golovinomyces orontii* infected Arabidopsis leaf epidermal cells expressing RPW8.2–YFP at 48 hours post-inoculation (hpi). The red box indicates the bleached area. White boxes 1 and 2 indicate a background area and a reference area of a haustorium in a neighboring cell in the same focal plane, respectively. Scale bars = 10 μm. Fluorescence intensities are shown with a false-color scale.
(b), (c) Scatter plots showing the individual half-time ($t_{1/2}$) and mobile fraction measurements for RPW8.2–YFP on haustoria at 24 (b) and 48 hpi (c). Each black dot represents data from one bleaching experiment. The horizontal lines indicate the mean half-time and mobile fraction values, based on data from 28 or 17 independent bleaching experiments at 24 and 48 hpi, respectively.
(d) Repetitive FRAP analyses based on bleaching the same region of the EHM three times (48 hpi). Images for pre-bleach, bleach and final recovery (555 sec) are presented with fluorescence intensities shown in a false-color scale. Scale bars = 10 μm.
(e) Fluorescence recovery curve showing fluorescence intensity at the apical EHM after three sequential bleaching events (data normalized using pre-bleach fluorescence intensities).

The recovery of fluorescence in the apical EHM was gradually attenuated after each successive bleaching over a time period of 30 min (Figure 6e). This suggests that recovery of fluorescence in the bleached apical region of mature haustoria largely originates through lateral membrane diffusion of RPW8.2–YFP from adjoining non-bleached EHM regions, rather than by vesicle-mediated replenishment. Taken together, our findings imply that vesicle-mediated trafficking of RPW8.2–YFP to the EHM occurs transiently during early haustorial development, whereas the lateral movement of RPW8.2–YFP protein within the EHM occurs at both early (24 hpi) and late (48 hpi) stages of haustorial development. This raises the possibility that the entire protein loading process must be initiated and completed within a narrow temporal window (Figure 7).

DISCUSSION

To exert localized resistance activity against powdery mildew fungi at the plant–fungal interface, it is essential for RPW8 to be properly targeted to the EHM (Wang *et al.*, 2009). However, the cellular trafficking machinery required for this specific transport of RPW8 to the EHM is completely unknown. To better understand the trafficking of RPW8.2 to the EHM, we took advantage of the compatible interaction between Arabidopsis and its host-adapted powdery mildew fungus *G. orontii*. Based on genetic and cell biological evidence, our study identified VAMP721/722 proteins as a component of the machinery required for transporting RPW8.2 to the EHM of *G. orontii* haustoria, the likely site for activation of resistance responses that eventually culminate in host cell death (Xiao *et al.*, 2001; Wang

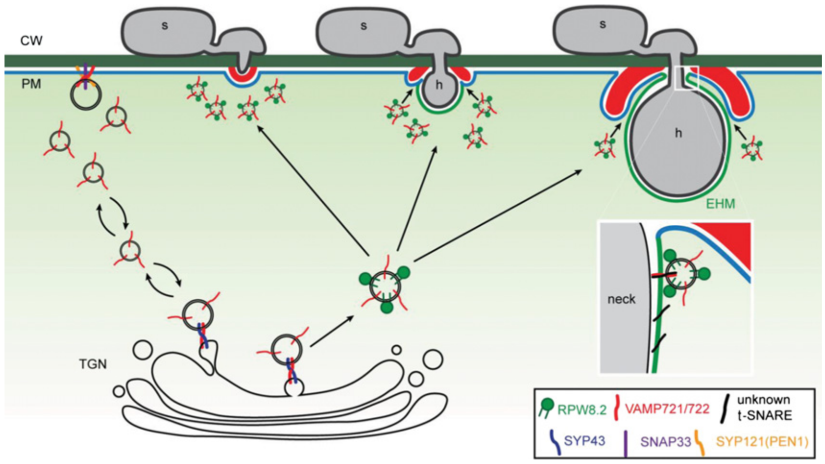

Figure 7. Schematic model of VAMP721/722 vesicle-trafficking for targeting RPW8.2 to the extrahaustorial membrane (EHM).
Since VAMP721/722 vesicles (red rods) partially co-localize with SYP43 protein (blue rods) at the *trans*-Golgi network (TGN) (Uemura *et al.*, 2012) and (Figure S8), these vesicles likely originate from the TGN. VAMP721/722 vesicles transport unknown cargos to exert pre-invasive immune responses against non-adapted powdery mildews at (or outside) the plant plasma membrane (shown in blue) in concert with SYP121/PEN1 (orange bars) and SNAP33 (violet bars) (Kwon *et al.*, 2008). Additionally, VAMP721/722 vesicles carry RPW8.2 (green bars) to exert anti-fungal defenses at the EHM as a post-invasive immune response against host-adapted powdery mildews. VAMP721/722 vesicles may use either a host or fungal t-SNARE (black bar) for specific proximal loading of RPW8.2 near the haustorial neck. At haustorial complexes, VAMP721/722 vesicles are incorporated into the encasement (labeled red), whilst RPW8.2 proteins are incorporated into the EHM (shown in green).

et al., 2009). We revealed that RPW8.2 proteins are transiently co-localized with VAMP721/722 proteins in infected epidermal cells during invasive growth of *G. orontii*, and are targeted to the EHM of haustorial complexes at 48 hpi. The conclusion that the trafficking of RPW8.2 protein is mediated by VAMP721/722 vesicles is strongly supported by genetic evidence that the resistance function of RPW8.2 protein depends on the gene dosage of *VAMP721* and *VAMP722*, and in particular *VAMP721*.

The closely related vesicle-resident VAMP721 and VAMP722 proteins were previously revealed as components of a ternary complex with plasma membrane-resident PEN1 and SNAP33 to restrict entry of the non-adapted powdery mildews *B. graminis* and *E. pisi* or macroscopically visible epiphytic growth of the host-adapted powdery mildew *G. orontii* (Kwon *et al.*, 2008) (Figure 7). Although we know that VAMP721/722 vesicles are partially co-localized with the TGN-resident Qa-SNARE SYP43 (Figure S9) and probably originate from the TGN (Uemura *et al.*, 2012 and Figure 7), the cargo molecules carried by VAMP721/722 vesicles remain enigmatic. Our subcellular localization data revealed that *G. orontii*-induced RPW8.2 proteins are carried on both VAMP721 and VAMP722 vesicles at an early stage of haustorial development (Figures 2 and 7). Since *vamp721 vamp722* double homozygous mutants show lethal seedling dwarf phenotypes, probably reflecting their requirement for cell plate membrane fusion during cytokinesis and secretory trafficking to the plasma membrane (Zhang *et al.*, 2011), both genes share redundant functions in development. Similarly, treatment with the elicitor-active epitope of bacterial flagellin, flg22, a microbe-associated molecular pattern (MAMP), stimulated enhanced seedling growth inhibition in both *VAMP721*$^{+/-}$ *VAMP722*$^{-/-}$ and *VAMP721*$^{-/-}$ *VAMP722*$^{+/-}$ plants (Yun *et al.*, 2013). Treatment with flg22 induces MAMP-triggered immunity (MTI) by activation of the membrane-resident FLS2 pattern recognition receptor, suggesting that during MTI plants prioritize the deployment of inducible VAMP721/722 secretory defense over plant growth. However, in the context of disease resistance triggered by live pathogens, the genetic functions of *VAMP721* and *VAMP722* appear to only partially overlap, with differential contributions to defense against different pathogen classes. For instance, only *VAMP721*$^{+/-}$ *VAMP722*$^{-/-}$ plants showed enhanced fungal entry into leaf epidermal cells with the non-adapted powdery mildew *E. pisi*, whereas *VAMP721*$^{-/-}$ *VAMP722*$^{+/-}$ plants were hypersusceptible to the virulent oomycete *Hyaloperonospora parasitica* (Noco2) (Kwon *et al.*, 2008). To further investigate the differential disease resistance functions of these two closely related VAMPs, we quantified the reproductive fitness of *G. orontii* on both haploinsufficient mutants. The susceptibility of *VAMP721*$^{+/-}$ *VAMP722*$^{-/-}$ plants to *G. orontii* at 10 dpi was more enhanced than that of *VAMP721*$^{-/-}$ *VAMP722*$^{+/-}$ plants (Figure 3a). In contrast, susceptibility of *RPW 8.2–YFP VAMP721*$^{-/-}$ *VAMP722*$^{+/-}$ plants to *G. orontii* at 10 dpi was much more enhanced compared with *RPW8.2–YFP* transgenic lines and *RPW8.2–YFP VAMP721*$^{+/-}$ *VAMP722*$^{-/-}$ plants (Figures 3b and 4c, d). Intriguingly, the activity of VAMP721/722 in disease resistance could be further differentiated by their cargo molecules: based on the analysis of trafficking efficiency of RPW8.2 proteins to the EHM, we revealed a major contribution of VAMP721 to RPW8.2 targeting, whereas VAMP722 plays only a minor role (Figure 5b, c). Notably, however, the localization of RPW8.2 on both VAMP721 and VAMP722 endomembrane vesicles upon *G. orontii* challenge (Figure 2) precludes a potential RPW8.2 cargo selectivity between the two vesicle types. It could be argued that the observed differential RPW8.2 targeting efficiency to the EHM is the consequence of RPW8.2-mediated resistance response activation prior to loading of the R protein onto the EHM. However, this is unlikely since loading of RPW8.2 onto the EHM is retained in *eds1* or *npr1* mutant backgrounds in which RPW8.2-dependent resistance activity is abrogated (Xiao *et al.*, 2001; Wang *et al.*, 2009). Instead we hypothesize that VAMP721- and VAMP722-dependent secretory machineries are targeted by pathogen effectors with differential efficiency to subvert plant secretory immune responses. Both haploinsufficient mutants display an essentially defeated pre-invasive disease resistance phenotype to the host-adapted *G. orontii* (Figure S3), suggesting that *G. orontii* interferes with differential effectiveness against VAMP721- and VAMP722-mediated post-invasive defense responses. Such a suppression of post-invasive plant immune responses was recently demonstrated for the host-translocated RXLR-type effector protein AVRblb2 of the oomycete pathogen *Phytophthora infestans*, which accumulates focally around haustoria and promotes virulence by interfering with the secretion of apoplastic papain-like defense proteases (Bozkurt *et al.*, 2011). Taken together, our findings imply the engagement of VAMP721, and with lower efficiency VAMP722, in a bifurcated trafficking pathway in which proteins are either carried to the plasma membrane for PEN1-dependent exocytosis or to the EHM for post-invasive defense (Figure 7).

Based on previous studies of subcellular responses to *G. cichoracearum* infection using a panel of fluorescent-tagged plasma membrane marker proteins, there are currently two hypotheses for biogenesis of the specialized EHM: the first proposes that the EHM develops through invagination and differentiation of the host plasma membrane, while the second proposes that the membrane is formed *de novo* by targeted secretion of specialized EHM-specific vesicles (Koh *et al.*, 2005). Previously an exosome biogenesis/release model was proposed, based on observations of the extracellular transport and integration of plant defense-related plasma membrane proteins, including PEN1 syntaxin, into pathogen-induced paramural cell wall compartments (Meyer *et al.*, 2009). However, the contribution of exosome-mediated secretion to EHM formation, if any, remains to be determined. Here, our findings implicate VAMP721/722 vesicle-mediated trafficking in the targeted secretion of RPW8.2 resistance protein to the EHM. Thus, the same R-SNARE-containing endomembrane vesicles become engaged for pre-invasive defense against non-adapted powdery mildews through complex formation with the plasma membrane-resident t-SNARE PEN1 syntaxin (Collins *et al.*, 2003; Kwon *et al.*, 2008) and for post-invasive defense against host-adapted powdery mildews by targeting the RPW8.2 resistance component to the EHM (Figure 7). For unloading the cargos of these vesicles at the EHM, we may postulate the existence of unknown alternative t-SNARE partners for VAMP721/722 docking and for EHM biogenesis, which are conceivably derived from either the host cell or the fungal pathogen. Since RPW8.2 trafficking is maintained in the *pen1*-1 mutant (Wang *et al.*, 2009), one scenario is that VAMP721/722 proteins may interact with another t-SNARE of Arabidopsis to secrete defense cargos at the EHM. One candidate is the plasma membrane-resident Arabidopsis t-SNARE SYP132, which was shown to interact both *in vitro* and *in vivo* with VAMP721/722 and is known to be required for plant development and resistance to pathogenic bacteria (Kalde *et al.*, 2007; Enami *et al.*, 2009; Yun *et al.*, 2013). Unfortunately, the failure to isolate Arabidopsis *syp132* mutants has hindered in-depth genetic studies with this t-SNARE. It is also possible that Arabidopsis v-SNAREs VAMP721/722 exploit a fungal t-SNARE for RPW8.2 trafficking to confer resistance to infection, assuming that fungal t-SNAREs can be translocated from the pathogen cell into the EHM.

To understand the identity and biogenesis of the EHM, there are a few interesting previous studies on dissecting the structure and composition of this membrane (Koh *et al.*, 2005; Micali *et al.*, 2011) and on defining the targeting motif analysis of RPW8.2–YFP (Wang *et al.*, 2013). Here, we were able to visualize the lateral mobility of RPW8.2–YFP protein within the EHM by FRAP analysis at 24 and 48 hpi. This revealed that fluorescence recovery in the bleached apical region of the EHM originates mainly from lateral diffusion of RPW8.2–YFP from adjacent non-bleached EHM regions rather than from *de novo* replenishment via RPW8.2–YFP-containing vesicles (Figures 6, S7 and S8). The lack of detectable post-bleaching replenishment of RPW8.2–YFP in the non-bleached EHM is unlikely to result from the activation of RPW8.2-mediated resistance responses, because loading of the protein onto the EHM is retained in an *eds1* mutant background in which RPW8.2-dependent defense activity is abrogated (Xiao *et al.*, 2001; Wang *et al.*, 2009). Instead, the progressive decrease of RPW8.2–YFP fluorescence in the non-bleached EHM at 48 hpi following consecutive photobleaching (for 30 min; Figure 6d) and the greater dynamics of RPW8.2–YFP at the EHM at 24 hpi compared with 48 hpi (Figure 6b, c) may point to the existence of only a narrow temporal window during which the entire loading process must be initiated and completed. Clearly, however, mobilization of RPW8.2 to the EHM is not strictly coordinated with the initiation of EHM biogenesis since *G. orontii* haustorium initials were frequently detected without detectable RPW8.2–YFP fluorescence at the EHM (Micali *et al.*, 2011). Nevertheless, pathogen-inducible *RPW8.2* gene expression and protein targeting to the EHM of powdery mildew haustoria is conceptually analogous to the coupling of arbuscular mycorrhizal fungus-induced transcription of *MtPT4* in *Medicago* root cells with the targeted loading of the encoded phosphate transporter into the peri-arbuscular membrane around arbuscules (Pumplin *et al.*, 2012). Our observations stimulate the future application of FRAP experiments with RPW8.2–YFP-expressing Arabidopsis plants to better define the location of protein loading onto the EHM of powdery mildew haustoria – for instance does this occur over the entire surface of the EHM or only via the haustorial neck region (Figure 7)?

EXPERIMENTAL PROCEDURES

Plant and fungal materials

Arabidopsis thaliana plants were grown as described previously (Kwon *et al.*, 2008). Plants used in this study were Col-0 as wild type, transgenic lines expressing RPW8.2–YFP, RPW8.2–RFP (Wang *et al.*, 2007), GFP-/mRFP–VAMP721 (Ebine *et al.*, 2011), mRFP–VAMP722, GFP–SYP43 (Uemura *et al.*, 2012) and the mutants *VAMP721*$^{-/-}$ *VAMP722*$^{+/-}$, *VAMP721*$^{+/-}$ *VAMP722*$^{-/-}$ (Kwon *et al.*, 2008) and *eds1*-2 (Aarts *et al.*, 1998). Arabidopsis Col-0 wild-type and both haploinsufficient mutants were used for generating transgenic plants expressing RPW8.2–YFP under 5′ regulatory sequences of RPW8.2. This plasmid was kindly provided by Dr Shunyan Xiao (Institute for Bioscience and Biotechnology Research, University of Maryland). Transgenic RPW8.2–YFP Col-0 plants were obtained as lines #1 to #4. Both haploinsufficient backgrounds of RPW8.2 transgenic lines were obtained as lines #14, #16, #21, #27 and #34. Polymerase chain reaction was used to validate the indicated genotypes for each experiment. To obtain transgenic plants with the same integration site for RPW8.2 expression in the haploinsufficient mutant backgrounds and in the Col-0 wild type, RPW8.2–YFP Col-0 transgenic lines #3 and #4 were crossed with both haploinsufficient mutants. The PCR-verified F_2 progeny siblings expressing RPW8.2–YFP in *vamp721* or *vamp722* single-mutant backgrounds or both haploinsufficient mutant backgrounds were used for conidiospore counts. To generate RPW8.2–YFP and mRFP–VAMP722 co-expressing plants, we crossed the respective transgenic plants.

Confocal laser scanning microscopy

All fluorescent tagged proteins were observed using either LSM 700 or LSM780 confocal microscopes (Carl Zeiss, http://www.zeiss.com/) equipped with a 40 × objective (C-Apochromat 40 × / 1.1 W). The YFP and mRFP were excited with 488 and 561 nm laser lines, respectively. For two-color imaging, multitracking was configured to avoid cross-talk between the fluorescence channels. The image data were processed using ZEN 2011 software (Carl Zeiss) and Adobe Photoshop CS5 (http://www.adobe.com/).

Pathogenicity assays

For enumerating fungal entry rates, 4-week-old plants were inoculated with *G. orontii* by brushing their leaves with heavily sporulating Arabidopsis leaves. Conidiospore counts were carried out as previously described with minor modifications (Wessling and Panstruga, 2012). Briefly, at least 12 4-week-old plants per genotype were evenly inoculated with *G. orontii* conidiospores using a settling tower and subsequently 300 mg of infected leaves from four plants were harvested as one sample. Three to four independent samples per genotype were used for conidiospore enumeration at the indicated time points.

Immunoblot analysis

Protein extracts from *G. orontii*-infected Arabidopsis leaves were prepared in SDS sample buffer and separated by SDS-PAGE on 10% gels and transferred onto polyvinylidene difluoride membranes for Western blots using anti-HSP70 (Stressgen SPA-817), anti-GFP (Clontech, http://www.clontech.com/) and anti-VAMP722 (Kwon *et al.*, 2008) antibodies. Immunoblots were visualized using a chemiluminescence detection system (LAS4000, Fujifilm, http://www.fujifilm.com/).

Fluorescence recovery after photobleaching experiments

We performed FRAP imaging on the EHM of *G. orontii* haustoria labeled with RPW8.2–YFP using an LSM780 confocal microscope (Zeiss) equipped with a 40× objective (C-Apochromat 40 × / 1.1 W) and a 514 nm argon ion laser for YFP excitation. For each FRAP experiment, two images was taken before bleaching, then the distal (apical) portion of the haustorium was bleached with 30 iterations at 100% laser intensity at 514 nm argon, after which a series of 40 or 80 images were captured at 15- or 10-sec intervals for 24 or 48 hpi, respectively. For each bleaching experiment, we collected the raw fluorescence intensity data for the target bleached area (red box, 5 × 3 μm), a reference area and a background area. The raw intensity dataset was normalized and used for fitting the recovery curve to a single exponential using the easyFRAP tool (Rapsomaniki *et al.*, 2012). Goodness-of-fit statistics (R-squares) for the 28 bleaching experiments at 24 hpi ranged from 0.54 to 0.99 and for the 17 bleaching experiments at 48 hpi, from 0.85 to 0.99.

ACKNOWLEDGEMENTS

We thank the following: Sabine Haigis for excellent technical support; Elmon Schmelzer for confocal microscopy assistance, Rainer Franzen for scanning electron microscopy; Chian Kwon for providing both haploinsufficient mutants and anti-VAMP722 antibody; Xunli Lu for helpful suggestions on the pathogenicity assay; Barbara Kracher and Girish Srinivas for the statistical analysis; Guillaume Robin for artwork in Figure 7; and Ryohei Thomas Nakano for critical reading of the manuscript. This work was supported by funds from the Deutsche Forschungsgemeinschaft Research Grant SPP1212 and by grants from the National Research Foundation (2010-220-C00039), Korea. The authors have no conflict of interest to declare.

SUPPORTING INFORMATION

Additional Supporting Information may be found in the online version of this article.

Figure S1. RPW8.2-RFP localizes to the EHM of *Golovinomyces orontii* haustoria.

Figure S2. Transient co-localization of RPW8.2–YFP with mRFP–VAMP722.

Figure S3. VAMP721/VAMP722 gene dosage does not affect pre-invasion resistance to *Golovinomyces orontii*.

Figure S4. Transgenic Arabidopsis plants expressing RPW8.2–YFP are more resistant to *Golovinomyces orontii*.

Figure S5. Expression levels of RPW8.2–YFP proteins in both haploinsufficient mutants and two single mutants.

Figure S6. Scanning electron micrographs showing epiphytic growth and sporulation of *Golovinomyces orontii*.

Figure S7. Fluorescence recovery after photobleaching analysis of RPW8.2–YFP dynamics at the extrahaustorial membrane of mature haustoria at 48 h post-inoculation.

Figure S8. Fluorescence recovery after photobleaching analysis of RPW8.2–YFP dynamics at the extrahaustorial membrane of young haustoria at 24 h post-inoculation.

Figure S9. Co-localization of VAMP721 and VAMP722 with SYP43 at the *trans*-Golgi network.

Methods S1. Transmission electron microscopy.

Methods S2. Scanning electron microscopy.

REFERENCES

Aarts, N., Metz, M., Holub, E., Staskawicz, B.J., Daniels, M.J. and Parker, J.E. (1998) Different requirements for EDS1 and NDR1 by disease resistance genes define at least two R gene-mediated signaling pathways in Arabidopsis. *Proc. Natl Acad. Sci. USA*, **95**, 10306–10311.

Bozkurt, T.O., Schornack, S., Win, J. *et al.* (2011) Phytophthora infestans effector AVRblb2 prevents secretion of a plant immune protease at the haustorial interface. *Proc. Natl Acad. Sci. USA*, **108**, 20832–20837.

Caillaud, M.C., Wirthmueller, L., Fabro, G., Piquerez, S.J., Asai, S., Ishaque, N. and Jones, J.D. (2012) Mechanisms of nuclear suppression of host immunity by effectors from the Arabidopsis downy mildew pathogen Hyaloperonospora arabidopsidis (Hpa). *Cold Spring Harb. Symp. Quant. Biol.*, **77**, 285–293.

Collins, N.C., Thordal-Christensen, H., Lipka, V. *et al.* (2003) SNARE-protein-mediated disease resistance at the plant cell wall. *Nature*, **425**, 973–977.

Ebine, K., Fujimoto, M., Okatani, Y. *et al.* (2011) A membrane trafficking pathway regulated by the plant-specific RAB GTPase ARA6. *Nat. Cell Biol.*, **13**, 853–859.

Enami, K., Ichikawa, M., Uemura, T., Kutsuna, N., Hasezawa, S., Nakagawa, T., Nakano, A. and Sato, M.H. (2009) Differential expression control and polarized distribution of plasma membrane-resident SYP1 SNAREs in *Arabidopsis thaliana*. *Plant Cell Physiol.*, **50**, 280–289.

Gil, F. and Gay, J.L. (1977) Ultrastructural and physiological properties of the host interfacial components of haustoria of *Erysiphe pisi in vivo* and *in vitro*. *Physiol. Plant Pathol.*,**10**, 1–12.

Kalde, M., Nuhse, T.S., Findlay, K. and Peck, S.C. (2007) The syntaxin SYP132 contributes to plant resistance against bacteria and secretion of pathogenesis-related protein 1. *Proc. Natl Acad. Sci. USA*, **104**, 11850–11855.

Koh, S., André, A., Edwards, H., Ehrhardt, D. and Somerville, S. (2005) *Arabidopsis thaliana* subcellular responses to compatible Erysiphe cichoracearum infections. *Plant J.*, **44**, 516–529.

Kwon, C., Neu, C., Pajonk, S. *et al.* (2008) Co-option of a default secretory pathway for plant immune responses. *Nature*, **451**, 835–840.

Lipka, V., Kwon, C. and Panstruga, R. (2007) SNARE-ware: the role of SNARE-domain proteins in plant biology. *Annu. Rev. Cell Dev. Biol.*, **23**, 147–174.

Maekawa, T., Kufer, T.A. and Schulze-Lefert, P. (2011) NLR functions in plant and animal immune systems: so far and yet so close. *Nat. Immunol.*, **12**, 817–826.

Martiniere, A., Lavagi, I., Nageswaran, G. *et al.* (2012) Cell wall constrains lateral diffusion of plant plasma-membrane proteins. *Proc. Natl Acad. Sci. USA*, **109**, 12805–12810.

Meyer, D., Pajonk, S., Micali, C., O'Connell, R. and Schulze-Lefert, P. (2009) Extracellular transport and integration of plant secretory proteins into pathogen-induced cell wall compartments. *Plant J.*, **57**, 986–999.

Micali, C., Gollner, K., Humphry, M., Consonni, C. and Panstruga, R. (2008) The powdery mildew disease of Arabidopsis: a paradigm for the interaction between plants and biotrophic fungi. *Arabidopsis Book*, **6**, e0115.

Micali, C.O., Neumann, U., Grunewald, D., Panstruga, R. and O'Connell, R. (2011) Biogenesis of a specialized plant-fungal interface during host cell internalization of *Golovinomyces orontii* haustoria. *Cell. Microbiol.*, **13**, 210–226.

Pumplin, N., Zhang, X., Noar, R.D. and Harrison, M.J. (2012) Polar localization of a symbiosis-specific phosphate transporter is mediated by a transient reorientation of secretion. *Proc. Natl Acad. Sci. USA*, **109**, E665–E672.

Rapsomaniki, M.A., Kotsantis, P., Symeonidou, I.E., Giakoumakis, N.N., Taraviras, S. and Lygerou, Z. (2012) easyFRAP: an interactive, easy-to-use tool for qualitative and quantitative analysis of FRAP data. *Bioinformatics*, **28**, 1800–1801.

Sarnowska, E.A., Rolicka, A.T., Bucior, E. *et al.* (2013) DELLA-interacting SWI3C core subunit of switch/sucrose nonfermenting chromatin remodeling complex modulates gibberellin responses and hormonal cross talk in Arabidopsis. *Plant Physiol.*, **163**, 305–317.

Spencer-Phillips, P.T.N. and Gay, J.L. (1981) Domains of ATPase in plasma membranes and transport through infected plant cells. *New Phytol.*, **89**, 393–400.

Takagi, J., Renna, L., Takahashi, H. *et al.* (2013) MAIGO5 functions in protein export from Golgi-associated endoplasmic reticulum exit sites in Arabidopsis. *Plant Cell*, **25**, 4658–4675.

Uemura, T., Kim, H., Saito, C., Ebine, K., Ueda, T., Schulze-Lefert, P. and Nakano, A. (2012) Qa-SNAREs localized to the trans-Golgi network regulate multiple transport pathways and extracellular disease resistance in plants. *Proc. Natl Acad. Sci. USA*, **109**, 1784–1789.

Wang, W., Devoto, A., Turner, J.G. and Xiao, S. (2007) Expression of the membrane-associated resistance protein RPW8 enhances basal defense against biotrophic pathogens. *Mol. Plant Microbe Interact.*, **20**, 966–976.

Wang, W., Wen, Y., Berkey, R. and Xiao, S. (2009) Specific targeting of the Arabidopsis resistance protein RPW8.2 to the interfacial membrane encasing the fungal Haustorium renders broad-spectrum resistance to powdery mildew. *Plant Cell*, **21**, 2898–2913.

Wang, W., Zhang, Y., Wen, Y., Berkey, R., Ma, X., Pan, Z., Bendigeri, D., King, H., Zhang, Q. and Xiao, S. (2013) A comprehensive mutational analysis of the Arabidopsis resistance protein RPW8.2 reveals key amino acids for defense activation and protein targeting. *Plant Cell*, **25**, 4242–4261.

Wessling, R. and Panstruga, R. (2012) Rapid quantification of plant-powdery mildew interactions by qPCR and conidiospore counts. *Plant Methods*, **8**, 35.

Xiao, S., Ellwood, S., Calis, O., Patrick, E., Li, T., Coleman, M. and Turner, J.G. (2001) Broad-spectrum mildew resistance in *Arabidopsis thaliana* mediated by RPW8. *Science*, **291**, 118–120.

Xiao, S., Brown, S., Patrick, E., Brearley, C. and Turner, J.G. (2003) Enhanced transcription of the Arabidopsis disease resistance genes RPW8.1 and RPW8.2 via a salicylic acid-dependent amplification circuit is required for hypersensitive cell death. *Plant Cell*, **15**, 33–45.

Yi, C., Park, S., Yun, H.S. and Kwon, C. (2013) Vesicle-associated membrane proteins 721 and 722 are required for unimpeded growth of Arabidopsis under ABA application. *J. Plant Physiol.*, **170**, 529–533.

Yun, H.S., Kwaaitaal, M., Kato, N., Yi, C., Park, S., Sato, M.H., Schulze-Lefert, P. and Kwon, C. (2013) Requirement of vesicle-associated membrane protein 721 and 722 for sustained growth during immune responses in Arabidopsis. *Mol. Cells*, **35**, 481–488.

Zhang, L., Zhang, H., Liu, P., Hao, H., Jin, J.B. and Lin, J. (2011) Arabidopsis R-SNARE proteins VAMP721 and VAMP722 are required for cell plate formation. *PLoS ONE*, **6**, e26129.